

Limit on the existence of $1/f$ noise in α decay

T. J. Kennett and W. V. Prestwich

Department of Physics, McMaster University, Hamilton, Ontario, Canada

(Received 21 February 1989)

A study is reported that was designed to search for the existence of a " $1/f$ "-noise component in the α -decay process. The experimental design was carefully optimized since simply attaining the Poisson variance limit is difficult when high-precision observations are made. Measurements indicate a "flicker floor" of $(2.1 \pm 3.7) \times 10^{-11}$. This result is not inconsistent with a complete lack of a $1/f$ component and is in marked contrast with an earlier reported value of 1×10^{-7} .

INTRODUCTION

Noise, or unpredictable changes in a quantity with time, can be conveniently characterized by the frequency dependence of its power spectrum. The most random, white or $1/f^0$ noise, is well understood both physically and mathematically. The integral of this noise yields $1/f^2$, or Brownian noise, which is associated with the random-walk process. While successive samples of white noise show no relationship or memory, the degree of correlation for $1/f^n$ noise increases with increasing n .

The most common and widespread type of noise found in nature displays a $1/f$ spectrum which can range over several decades. This noise, referred to as flicker noise, arises in most semiconductor devices, atomic and quartz clocks, as well as in such diverse domains as ocean, traffic, and hourglass flows. Music and some art forms also reveal a similar power spectrum. While flicker noise is omnipresent, the physical origins remain uncertain. A potential clue is that it is possible to synthesize $1/f$ behavior by processing white noise with a distribution of time constants. Barnes and Jarvis¹ have developed an algorithm which produces such a transformation. They show that with five RC filters a $1/f$ power spectrum is obtained which spans four decades.

A theory has been proposed by Handel^{2,3} in which he attempts to establish a unifying principle for $1/f$ noise. In this quantum theory, charged particle motion is coupled to infrared quanta emitted as bremsstrahlung. The quanta have a number spectrum which varies as $1/f$. Self-interference or quantum beats between components of slightly different energies is shown to produce $1/f$ fluctuations in particle currents. While objections to Handel's derivation have been raised, experimental results in electron-scattering phenomena and mobility fluctuations agree with the theoretical predictions.⁴ Application of the theory to emission processes, in particular α decay,³ has met with mixed reaction. Now some doubt regarding both the theoretical derivation given by Handel and certain supporting experimental findings has surfaced.

The emission theory predicts³ that the rate of α -particle decay is subject to $1/f$ fluctuations. This implies that the decay process will display rate fluctuations in excess of that associated with the Poisson distribution. The

additional contributor, as formulated,⁵ will have the effect of introducing a finite limit to the relative precision that can be obtained as the number of counts acquired is increased indefinitely. The ultimate precision attainable is referred to as the flicker floor with the magnitude, estimated to be 10^{-7} ,⁵ indicating the contribution of $1/f$ noise to the emission process. Since this theory was proposed, several critiques have been forthcoming.⁶⁻⁸

A group of investigators has reported observation of a finite flicker floor in radioactive α decay.⁹⁻¹¹ The experimental results, which corroborate the predictions of van Vliet and Handel,⁵ reveal flicker floors in the neighborhood of 10^{-7} . Recently the validity of these experimental findings has been challenged.¹²⁻¹⁴

Initially Gong *et al.*⁹ reported a departure from Poissonian statistics that would correspond to a flicker floor of 10^{-7} . The measurement involved the use of a ²⁴¹Am source and a surface barrier detector. Shortly after this result was reported, Prestwich *et al.*¹² examined the statistics of the γ -ray emission following α decay of ²⁴¹Am. These authors observed no departure from Poissonian counting statistics and were able to set the upper limit for a flicker floor some two orders of magnitude lower than that observed by Gong *et al.*⁹ This discrepancy implied that either a difference exists between the two emission processes, which are highly time correlated,¹³ or that the α -particle measurements of Gong *et al.* were corrupted by unknown instrumental effects. Since one is dealing with variances, the presence of any spurious effects will inhibit the attainment of the Poisson limit.

To ensure that these contradictory outcomes could not be associated with the fact that the monitored emissions were different, an experiment using the same arrangement as Gong *et al.*⁹ was undertaken by Pepper *et al.*¹⁴ Their results again showed no departure from the Poissonian outcome and permitted them to establish an upper limit for the flicker floor of 2×10^{-9} . This again demonstrated that the earlier observation⁹ does not reflect the presence of a $1/f$ contribution in α decay.

Recently the group that first reported the existence of a finite flicker floor have concluded a wider-ranging study.¹¹ Using α -ray sources of ²³⁹Pu, ²⁴¹Am, and ²⁴⁴Cm these authors again observed flicker floors in the region of 10^{-7} . In the case of measurements involving mixtures of

these and other isotopes, very significant deviations from the Poissonian result were observed. The form of the recorded departures was not indicative of a $1/f$ component so Lorentzian noise was invoked in an attempt to explain the results. While possible chemical processes within the sources which could affect the solid angle are suggested and discussed, a critical examination of experimental and spectral analysis techniques may have been more fruitful. In their work¹¹ the authors conclude that the departures they observe reflect the presence of a $1/f$ component and that in certain instances a source related process is operative. Clearly only the former is of fundamental importance otherwise the results may well be attributable to experimental design and sample preparation technique.

The contention that counting statistics may not be solely Poissonian has implications for metrology and for our understanding of the decay process. Presently the evidence against the existence of a $1/f$ contribution is reasonably strong. However, the upper limit should be reduced to the point where, in any practical situation, a $1/f$ contribution would be negligible. On other grounds a reduced limit could assist in resolving the controversy concerning the emission theory.³ These factors prompted us to undertake the present study.

EXPERIMENTAL CONSIDERATIONS AND DESIGN

Observation of a $1/f$ component in a decay process requires measurement of counting rate variation through the use of the variance or a related quantity. Unfortunately $1/f$ noise yields a variance that diverges with number of samples and so it is common practice to use the Allan variance^{15,16} or the mean-squared successive difference, which avoids this difficulty.

Both the normal and Allan variance will indicate signal variation whether it be spurious or real, therefore, the apparent flicker floor will reflect the care with which an experiment is designed and conducted. Under ideal experimental conditions the limit that can be established is approximately equal to the reciprocal of the total number of events acquired. To make a meaningful contribution, we felt that the experimental must have the capability to sense a flicker floor in the region of 10^{-11} . The need for a combination of high counting rates and long counting periods to attain the limit objective prompted us to undertake an examination of all relevant experimental factors.

Because the theory and supportive work relate to α decay, an experiment to investigate this type of radiative process was planned. Instrumental instabilities or drifts usually display a $1/f$ power law¹⁷ and so an attempt was made to identify the factors which contribute to system stability and to assess their relative importance.

Usually α -ray spectrometry is conducted using a solid-state detector mounted within an evacuated chamber. The source, placed some distance from the detector, is made as thin as possible. Data are acquired and the rate determined by integration of a preselected region of the spectrum. With such a system, variation in counting rate can arise because of a variety of factors. These can be

conveniently traced to changes in temperature and pressure where consideration of effects must be placed in a context consistent with the limit objective set.

Temperature changes can affect electronic components and hence the system gain which makes reproducible spectral area measurements difficult to attain. Possibly of more importance is the fact that dimensional changes of two parts in 10^5 per $^{\circ}\text{C}$ can occur. The actual change in solid angle and hence counting rate will depend upon the configuration of the counting chamber and the construction materials used. Temperature changes tend to show a diurnal variation and, if such an effect is present, one can expect large departures from the expected Poissonian statistics.

The constancy of pressure within a counting chamber determines both the number of events detected (nuclear scattering) and the form or detailed shape of the spectrum (straggling). Since these two factors influence the estimated rate, pressure effects will enter on both accounts. With a simple pumping system, ambient pressure changes will be reflected differentially within the chamber. Based upon geometry, pump quality and the spectral analysis technique used, pressure changes could impede reaching the desired sensitivity.

Finally, the possibility of charge buildup on the source and local structure must be considered. In the absence of strong grounding it is plausible that stray fields could alter the effective solid angle sufficiently to produce rate changes of the order of the precision goal we have set. The inherent problems and potential limitations associated with this common method of conducting α -ray spectroscopy prompted us to seek another alternative.

Unlike the method of α -particle assaying based upon the solid-state detector, scintillation counting can usually handle significantly higher counting rates. To attain the statistical precision desired, this rate property is essential. With the scintillation method only some of the effects discussed above remain and these are at diminished levels of importance.

An attractive approach for the proposed measurement appeared to be the incorporation of an α -ray emitter into the scintillator itself. Once mounted to the photomultiplier, there is little possibility for rate changes because of solid-angle effects traceable to temperature and pressure variation. While light output might certainly change because of radiation damage, the number of events occurring should not. Thus only gain effects and changes in spectral form must be addressed. Because it is not possible to reduce the expectation value of the variance, except through dead-time effects, the test of this approach or any other method rests in the quality of data that can be obtained.

EXPERIMENTAL ARRANGEMENT, CONSIDERATIONS, AND EXECUTION

The experimental arrangement is illustrated in Fig. 1. The radiation source consisted of approximately 10 kBq of ^{241}Am which was incorporated into the lattice of a NaI(Tl) crystal. The crystal with the dopant activity, a subsystem of a NaI light pulser, was prepared and packaged by the Harshaw Chemical Company. The unit is in

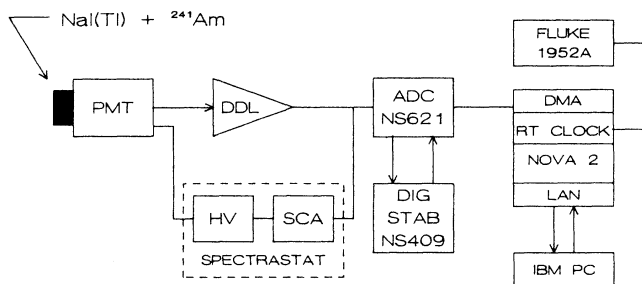


FIG. 1. Experimental arrangement.

the form of a right cylinder of height $\frac{3}{8}$ in. and diameter $\frac{1}{4}$ in., with an optical window which was coupled to a Hamamatsu R 647 1-cm-diam photomultiplier tube. The actual scintillation crystal is rectangular with height $\frac{1}{16}$ in. and lateral dimensions $\frac{1}{8} \times \frac{1}{8}$ in.²

The γ -ray equivalent energy for the 5.48-MeV average α -particle energy of ²⁴¹Am was found to be approximately 4 MeV. This high equivalence is a valuable attribute since it ensures that the apparent energy of the events of interest is well above that for common background radiations. In addition, the dimensions of the scintillator restrict the maximum possible energy deposition by electrons to a value well below 2 MeV. Based upon the volume of the scintillator, about 0.016 cm³, an estimated unshielded background rate of 0.016 cps was deduced from data obtained with a 1×1 -in.² NaI(Tl) crystal placed in the same environment.

The output from the photomultiplier was conditioned by a preamplifier and a 2011 Canberra amplifier. The relatively high counting rate necessitated the use of a 0.5- μ sec clipping time to reduce the occurrence of random adding. Also because of the rate the bipolar output was selected for encodement by a 50 MHz Northern Scientific NS621 analog-to-digital converter (ADC). To minimize dead time, the converter was operated with a ramp of 256 channels.

The ADC is coupled in a parallel fashion to a Data General NOVA2 minicomputer via the data channel. This link permits word transfers to be completed within a machine cycle, or about 1 μ sec. A NOVA2 assembly language program controls all aspects of the acquisition process. In addition it provides spectral display and parameter information during the experiment. The NOVA2 collects and sorts ADC events for a time interval selected by the investigator and at the finish of this period, the acquired data are transferred to an IBM PC. The gathered resident information is then erased and another cycle started.

Transfer of spectral data to the PC is initiated by the NOVA2 and is conducted using a serial communication system devised for this purpose. The transfer rate is 2.5 megabits per sec with echo checking, and, in the event that an error is detected, the data are retransmitted. The entire readout and reinitiate cycle takes 3 sec to complete. Following a valid transfer, the PC writes the data to a floppy disk. The NOVA2 stores the data in the form of 32-bit integer words and to hasten the transfer and to

optimize storage the long integer format was used by the PC. Each record requires 1 kbyte hence 354 records can be placed on a single disk. In addition to the 256-channel spectrum and record number, the clock and live time are included.

The time base was derived from the 1.5-MHz crystal controlled clock of the NOVA2. Control of the acquisition cycle and monitoring of the dead time relied upon the scaled 100 Hz real-time clock of the NOVA2. Dead time was sensed by ANDing the scaled clock with the busy signal of the ADC. Because the investigation is based upon the constancy of the clock period and because such clocks are known to drift,¹⁵ the fundamental was monitored with a Fluke 1952A counter. Throughout the 30-week duration of this study no net drift in frequency was observed even though significant temperature changes did occur. Variation about the mean frequency amounted to about 1 part in 10^7 , a value characteristic of crystal-controlled oscillators.

Previous studies showed that gain instability is mainly attributable to the temperature dependence of the photomultiplier. To reduce this, a Cosmic Spectrstat was employed. The high voltage obtained from this module is controlled by the pulse amplitude of a selected spectral component. The offset of a single-channel analyzer, centered at the selected peak, is modulated so that the window alternately samples each side of the peak. Any misbalance introduces an error signal which is used to alter the high voltage in the appropriate direction. This system ensures a relatively constant gain signal to the output of the spectroscopic amplifier.

Further and finer stabilization was employed at the encodement segment through use of a digital stabilizer, an NS409, working in conjunction with the ADC. Here the gain of an input stage to the ADC is controlled by movement in the centroid of a digitally selected region of the spectrum. Provided that the input gain does not change by more than a few percent, this system will ensure constancy of the digitized information. Throughout the study, the digital window was centered about the full-energy peak of the α -particle spectrum shown in Fig. 2. No zero-point stabilization was employed.

Dead time

The system gain was selected so as to place the full-energy peak near the midpoint of the 256-channel range. Preliminary measurements indicated that a mean dead time of about 7% would be encountered with the 10^4 -cps input rate and this gain. The importance of a stationary dead time when high-precision studies are made can be quantitatively assessed by considering the following example. In a 4-min counting period 2.4×10^6 events will occur and about 2.24×10^6 will be recorded yielding an uncertainty of some 1500. If the 7% dead time changes by 1% to 7.07%, the number of events recorded will change by about 1600, an amount exceeding the statistical uncertainty.

To identify the components which contribute to dead time, a series of measurements was conducted. Here the output from the detector system was used to trigger a

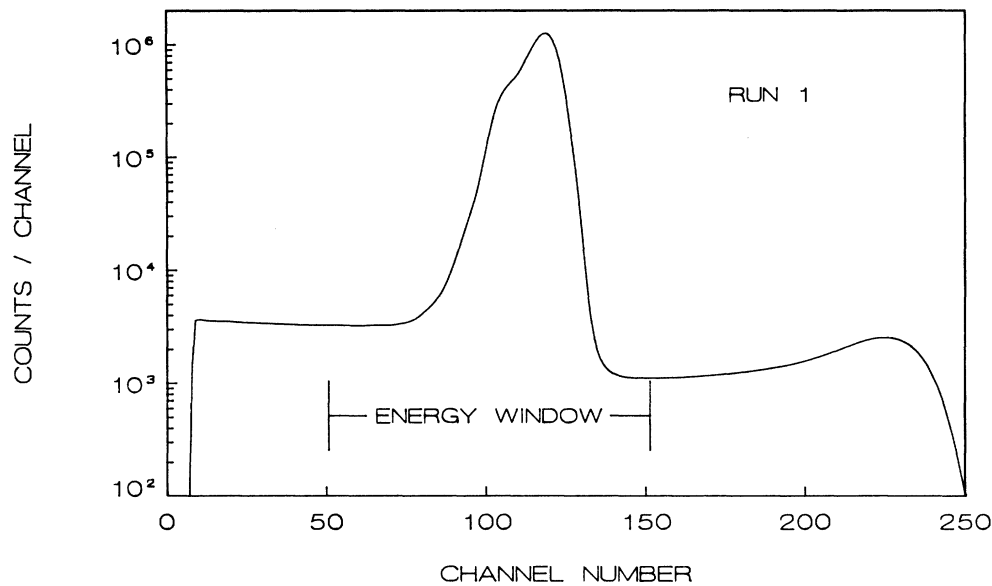


FIG. 2. α -particle spectrum obtained with a doped scintillator. Complete energy deposition is reflected by the peak at channel 115. The spectrum above this peak corresponds to random-adding events. In the treatment of the data, the spectral area was taken to be either the total as displayed or that within the indicated energy window.

BNC PB-3 pulser thereby generating constant amplitude, time-distributed events. These pulses were then processed by an amplifying system adjusted so as to match the output waveform of the detector. Encodement and storage of such signals allowed determination of the mean pulse height, $\langle I \rangle$ channels. An estimate of the dead time τ_α was obtained from the recorded clock and live time. By selecting some ten values for the pulser amplitude, the relationship

$$\tau_\alpha = 4.5 + 2 \times 10^{-2} \langle I \rangle \quad (1)$$

in μsec , was found. Here the constant term consists of the average asynchronous service time in the data channel, about $1.5 \mu\text{sec}$ and a nominal $3\text{-}\mu\text{sec}$ delay in opening the ADC linear gate after an event has been processed. The latter is a feature included in the design of the ADC. While the large constant term makes the dead time less dependent upon system gain, the importance of its stability increases. For the principal runs, which had a value $\langle I \rangle = 114.1$ channels, the live-time measurement indicated that the average dead time per event was $1.8 \mu\text{sec}$. This is in agreement with the result predicted by evaluation of Eq. (1).

Although the dead time of the ADC is monitored at 100 Hz, uncertainty exists because the dead time is a binomially distributed quantity. For example, in a 30-min counting interval the uncertainty in the estimated dead time is about 0.3%. When the dead-time correction is made, this uncertainty translates to an error that is comparable to the statistical error for a 30-min count. The relatively low correlation between measured dead time and total counts makes detection and therefore adjustment for any real dead-time changes impractical. On the other hand, by simply determining the mean pulse height

for each spectrum, the actual dead time can be obtained without error by application of Eq. (1). While there is no statistical uncertainty, the accuracy does depend on the constancy of the parameters in Eq. (1).

Preliminary studies failed to reveal any decay in the mean counting rate although statistically this should have been observed. In fact, in some cases the rate was observed to increase with time. While the location of the central portion of the full-energy peak appeared stationary because of the stabilization used, the mean pulse height was found to display a slight drift toward lower values with time. This effect reduced the dead time sufficiently to just compensate for the radioactive decay. The principal reason for this lowering of the pulse height was found to be due to a very small change in the response function. This change was traced to physical movement of the scintillator on the phototube face. Redesign and reconstruction of the mounting eliminated this effect.

The present study did reveal, at its completion, that the phototube was beginning to show measurable aging effects. This is not surprising in view of the fact that some 2×10^{12} α -ray events/cm² has occurred. The mean pulse height proved to be a very sensitive measure of subtle changes in response function, and is therefore a useful quantity to monitor.

By noting the recorded dead time and evaluating the mean pulse height for each spectrum acquired, the presence of any long-term drifts can be sensed. Throughout both major runs, each spanning intervals of about 6 weeks, no discernible variation was detected in these quantities. The first run consisted of 1696 30-min samples while the second was composed of 2048 such samples. Both runs were terminated because of equipment failure.

Random adding

Figure 2 shows the spectrum obtained through averaging 354 30-min records. The figure reveals that the resolution realized is about 10%. The spectral form is relatively simple with the presence of random adding clearly visible above the full-energy peak. This summed component arises when the system analyzes a pulse pair whose time difference falls within the amplifier resolving time.

A quantitative assessment of the random-adding contribution was made by mixing the output of a BNC PB-7 pulser and the photomultiplier signal within the preamplifier. Selection of appropriated gains for the two components permitted generation of the spectrum shown in Fig. 3. The response and frequency of the pulser was determined in order to evaluate the magnitude of the random-adding component. The value obtained, 1.5%, agrees with what one expects from the counting rate and the amplifier response [full width at half maximum (FWHM) 1.0 and base width of 1.5 μsec].

The presence of triple-pulse addition can be sensed because of the total lack of background in the energy region above 8 MeV. The contribution of events displaying an amplitude of less than that of the pulser arise because of the bipolar pulse used. If the random-adding events are included in the summation of total events, without any numerical weighting, their true contribution will be incorporated by any dead-time corrections that is applied. This is assured because the average dead time of 6.8 μsec is greater than the 1.5- μsec resolving time for random adding.

Data monitoring and analysis

Several possible approaches exist to analyze digitized spectra for which a measure of area is desired. In the

present study two methods were used. Neither of these was applied until it had been established, for each spectrum in the sequence of runs, that the gain, the dead time, the mean pulse height, and the lower-level cutoff remained unchanged in a statistical sense.

The gain was determined through use of a smoothed, second-order filter¹⁸ applied to the full-energy peak in order to deduce its centroid. Because this procedure affects bandwidth, the results will differ from the mean pulse height estimate when spectral shape changes. Consequently, to protect against small changes in the system response function going undetected, the mean pulse height was also determined.

The lower-level cutoff, which is established by the ADC, controls the acceptability of pulses for analysis. The stability of this level directly affects the number of events accumulated. This quantity was monitored by determining that the first recorded channel retained, within error, the same value. Throughout both runs, all four monitored quantities remained constant, within their respective statistical error.

The first method of intensity analysis consisted of simply integrating the total recorded spectrum. For the remainder of this paper, results obtained with this treatment will be referred to as a total sum.

An examination of the recorded spectrum, shown in Fig. 2, reveals that large spans above and below the full energy peak display a relatively constant intensity with the upper region containing the lower value. This disposition suggested that it may be possible to choose summation channel limits that would make the selected area independent of gain change. If, for example the gain increases while the integration limits remain at fixed channels, the area gained at the lower bound may just equal that lost at the upper limit.

Consider the case where the area of a spectrum $S(x)$

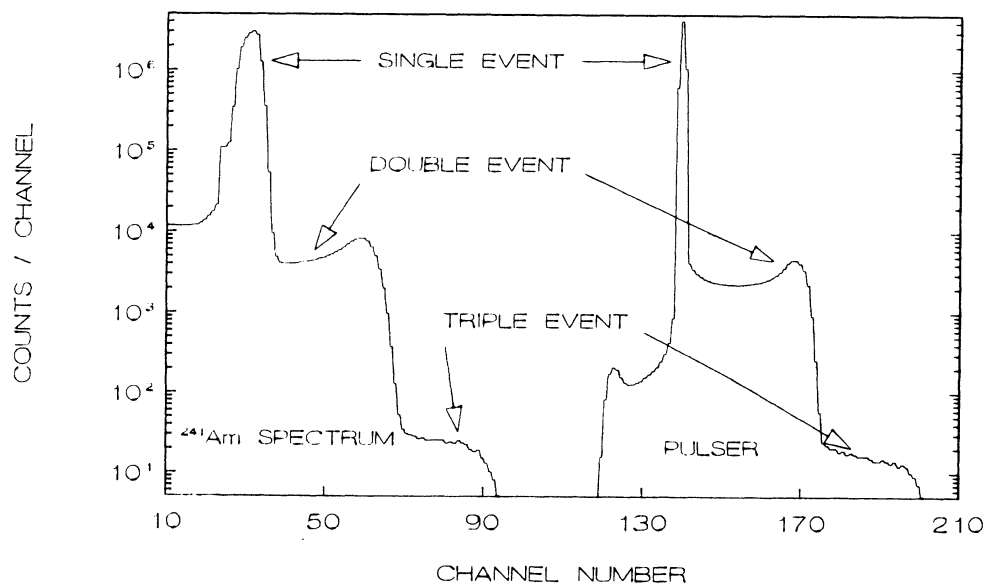


FIG. 3. α spectrum showing the occurrence of multiple random adding is presented at low channel number. The spectrum at the upper channel region is that obtained using a pulser and represents the response function for random adding.

within the channel bounds x_1 and x_2 is to be determined. If the system gain changes by the factor $(1+\beta)$ while the integration limits remain fixed, the limits based upon the unaltered spectrum will in effect be reduced by the factor $1/(1+\beta)$. The change in area can be written, using a Taylor expansion about these limits, as

$$\int_{x_1/(1+\beta)}^{x_1} S(x)dx - \int_{x_2/(1+\beta)}^{x_2} S(x)dx \approx \frac{\beta}{(1+\beta)} [x_1 S(x_1) - x_2 S(x_2)] + \frac{\beta^2}{2(1+\beta)^2} [x_1^2 S'(x_1) - x_2^2 S'(x_2)], \quad (2)$$

yielding second-order independence from β via the conditions

$$S(x_1)/S(x_2) = x_2/x_1$$

and (3)

$$x_1^2 \frac{dS}{dx} \Big|_{x_1} = x_2^2 \frac{dS}{dx} \Big|_{x_2}.$$

As can be seen from the spectrum in Fig. 2, the rather constant regions above and below the peak are in height ratio of about 3 to 1 with almost zero slope. Selection of limits to obtain maximum area and second-order independence from gain changes indicate channel number limits of $x_1 = 50$ and $x_2 = 150$. Numerical treatment of the spectrum revealed the best choice to be channels 51 and 150. This range is indicated in Fig. 2 and, for data analyzed by this second method, the term window sum

will be used.

Finally correction for radioactive decay must be considered. While the ^{241}Am half-life of 432 yr Ref. 19 would normally be considered long enough to ignore, the high precision obtained here requires a correction. To illustrate this the total area data for run 2 are shown in Fig. 4. Here the data have been gathered to produce 16 terms, each of 64-h duration. Based upon the mean counting rate of 3.7×10^7 counts/h, one expects that each entry will decrease by 0.57 of the standard deviation, that is about 2.8×10^4 counts in a total of 2.4×10^9 . This is confirmed by the results given in Fig. 4 where the expected change in counts with time, based upon the half life, is shown by the line. The observations are statistically in agreement with the prediction.

OBSERVATIONS AND THEIR TREATMENT

Initially, the data from the two runs and some shorter duration results were analyzed in a manner similar to that used by previous authors.¹ The Allan variance for adjacent observations, X_1 and X_2 , is given by

$$\sigma_A^2 = 0.5(X_1 - X_2)^2 \quad (4)$$

and for r terms

$$\sigma_A^2 = \frac{1}{2(r-1)} \sum_{i=1}^r (X_i - X_{i+1})^2. \quad (5)$$

The case where Poissonian and $1/f$ noise appear in an emission process has been treated⁴ with the result that the relative Allan variance $R(T)$ may be expressed as

$$R(T) = \sigma_A^2 / (m_0 T)^2 = 1 / (m_0 T) + 2C \ln(2). \quad (6)$$

Here m_0 is the mean counts per unit time, T is the counting time, and C the strength or power of the excess noise, $S(f)/m_0^2$. From (6) it is seen that as $T \rightarrow \infty$, $R(T) \rightarrow 2C \ln(2)$. The existence of a "flicker floor" is most easily seen graphically when $R(T)$ is plotted against $1/T$.

Before any data can be examined, correction for dead-time losses is necessary since this effect suppresses both the variance and the Allan variance. While the dead time has been determined, the nature of the loss mechanism has not. In general one considers the limiting models of paralyzable (type 1) and nonparalyzable (type 2) systems.²⁰ Fortunately it is possible to derive a relationship for the variance obtained with a system that is between the two extreme models. If P is the probability that the system is paralyzable, then the relation between the observed rate R_{obs} and the true rate R is given by

$$R_{\text{obs}} = PR / [P - 1 + \exp(PR\tau)], \quad (7)$$

where τ is the dead time per event. After some manipulation the ratio of the observed variance to the observed mean can be written as

$$\sigma^2/M = [Z(Z - 2PR\tau) + P^2 - 1] / (Z + P - 1)^2, \quad (8)$$

where $Z = \exp(PR\tau)$. The quantity defined in Eq. (8) indicates the degree to which the ratio, which is unity for a lossless Poisson process, is dampened because of dead

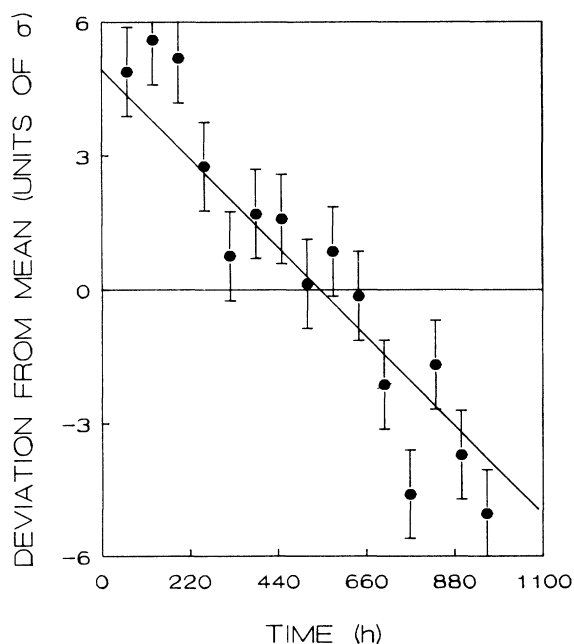


FIG. 4. Mean value for run 2 using 64-h counting intervals. The line displays the decay trajectory expected for 432-y ^{241}Am . The ordinate is given in units of the standard deviation.

time. The values for τ and R were established experimentally but that for P was not. Evaluation of Eq. (8) for P in the range from 0 to 1 for the case at hand yielded values of 0.873 and 0.869, respectively. Because all measurements are corrected by the same factor, the choice of model will have little effect upon the final outcome. Correction of the Allan variance is therefore virtually independent of the exact nature of the system dead time.

The dependence of the Allan variance on counting period can be explored by acquiring measurements of varying duration or by gathering a set of fixed-period observations into subsets. Taking the latter approach, the 30-min data were gathered into even larger groupings. Nominally each regrouping compressed the number by a factor of 2 thereby increasing the time span by 2. The validity of this approach hinges upon the degree of correlation that exists between the synthesized sets. This will be examined in detail and its validity demonstrated below.

A correction of about 14% was applied to account for the dead-time effect in the relative Allan variance $R(T)$. The results obtained for both runs are shown in Figs. 5 and 6. Here the data have been divided, respectively, into window and total integration for area determination. Also indicated are the results of the previous investigators.⁹ Both figures fail to reveal any evidence for the existence of a constant term but rather support the expected Poisson relationship. While a quantitative analysis of the results in these figures is possible, the correction for counting losses made such an option unattractive. Instead, the problem was reconsidered with the objective of obtaining a limit for the flicker floor that would be in-

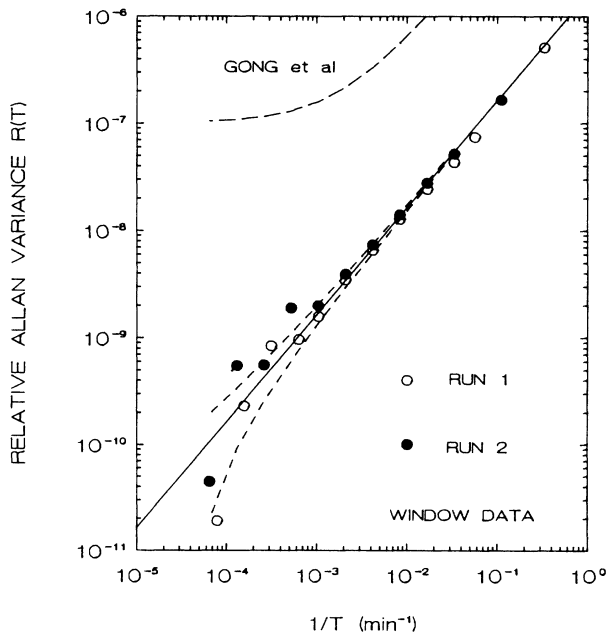


FIG. 5. Relative Allan variance $R(T)$ is shown as a function of the reciprocal of the counting time T for the energy window area. The results of Ref. 9 are also shown. The dashed lines show the deviation expected for the number of samples used.

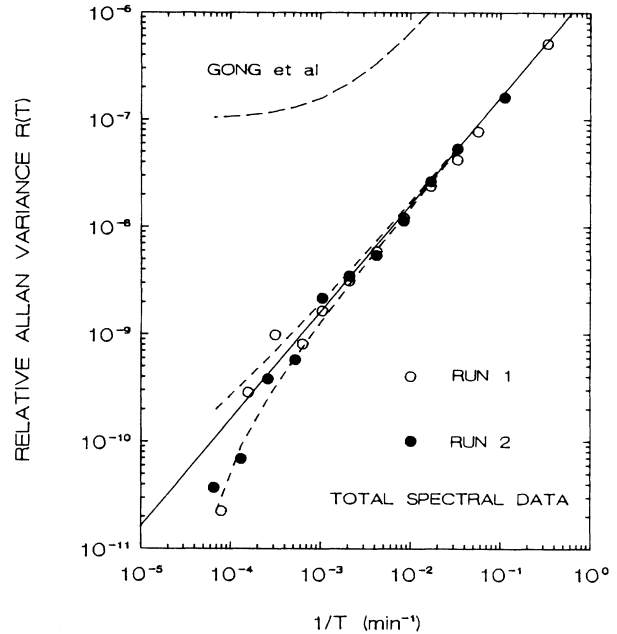


FIG. 6. The results obtained when the total area is used are shown. Notations are as in Fig. 5.

dependent of counting rate and counting system.

In the treatment of $1/f$ noise associated with the frequency of clocks, Barnes¹⁵ examined the nature of signal variance. Given that a signal has spectral power density C/f , he showed that the expectation value of the variance for N adjacent samples is

$$\langle \sigma^2(N) \rangle = N \ln(N)C / (N - 1) . \tag{9}$$

Here that value of σ^2 for N samples of the signal X_i is found in the usual way via

$$\sigma^2(N) = \sum_i^N (X_i - \langle X \rangle)^2 / (N - 1) . \tag{10}$$

From Barnes's derivation the expectation value for the mean-square successive difference which, unlike the variance, is bound has the value

$$\langle \sigma^2(2) \rangle = 2 \ln(2)C \tag{11}$$

where

$$\sigma^2(2) = \sum_1^{N-1} (X_i - X_{i+1})^2 / [2(N - 1)] . \tag{12}$$

This latter quantity is, in the field of $1/f$ noise, termed the Allan variance. In statistics the term mean-square successive difference is used with the factor two deleted from the denominator. Equations (9) and (11) show that the coefficient of the power density C is dependent upon which variance is computed. For the present study both $\sigma^2(2)$ and $\sigma^2(N)$ are dampened due to dead time but, by taking their ratio, a statistic independent of this effect is obtained. In the event where both Poisson and $1/f$ noise are present, these variances are given by

$$\sigma^2(2)/M^2 = 1/M + 2 \ln(2)C \quad (13)$$

and

$$\sigma^2(N)/M^2 = 1/M + N \ln(N)C / (N-1). \quad (14)$$

Here $F = 2 \ln(2)C$ which represents the "flicker floor" as used by Ref. 7 and M is the average total count associated with each of the N datum. Defining Γ to be

$$\Gamma = [\sigma^2(2)/\sigma^2(N)] - 1 \quad (15)$$

and solving Eqs. (13) and (14) for C yields

$$C = \frac{\Gamma}{M[2 \ln(2) - (\Gamma + 1)N \ln(N)/(N-1)]}. \quad (16)$$

For a Poisson process devoid of any 1/f component Γ , and hence C , is zero. The error associated with C depends only upon that in Γ . The statistic Γ has been discussed by several authors^{21,22} and is sometimes referred to as the Durbin-Watson parameter. Williams²³ proved that the second moment of Γ is in fact equal to the ratio of second moments of $\sigma^2(2)$ and $\sigma^2(N)$ which, for normally distributed data are, respectively,

$$1 + \frac{3N-4}{(N-1)^2}, \quad 1 + \frac{2}{(N-1)}. \quad (17)$$

The value for σ^2 is thus $(N-2)/(N^2-1)$. The uncertainty in C , determined via error propagation for the case where $\Gamma \approx 0$, is

$$\sigma_C^2 = \frac{N^2(N-2)}{Q^2(N^2-1)[N \ln(N)/(N-1) - 2 \ln(2)]^2}. \quad (18)$$

Here Q is the total number of counts accumulated in the experiment.

In the present study, a large number of observations were made in order that they could be concatenated to provide several subsets. Consider that n observations are made, each consisting of a single measurement, i.e., $m = 1$. These may be gathered into a set of $n/2$ elements through adding consecutive datum giving $m = 2$. The number of elements in the set is $N = n/m$ and the average count for an element is $M = Q/N$.

At first glance it might appear that the correlation between the gathered sets is so high that little new information can be obtained through their use. To explore this, an algebraic evaluation was carried out to determine the correlation coefficients of $\sigma^2(2)$ and $\sigma^2(N)$ for various degrees of concatenation. It is found that, when the observations are described by normal variates, the correlation coefficient for sets i and j , $r_{ij} = \sigma_{ij}^2 / (\sigma_i^2 \sigma_j^2)^{1/2}$, can be written for $\sigma^2(2)$ as

$$r_{ij} = (1/j)(2N/j - \frac{4}{3}) / [(2N/i - \frac{4}{3})(2N/j - \frac{4}{3})]^{1/2}. \quad (19)$$

Here the indices (i, j) are equal to the m values associated with the two data sets and $i < j$. If the number of elements in the set N is much larger than unity Eq. (19) reduces to simply

$$r_{ij} = (i/j)^{3/2}. \quad (20)$$

For $\sigma^2(N)$ the corresponding result is

$$r_{ij} = (i/j)^{1/2}. \quad (21)$$

For the present approach interest resides in how the correlation coefficient associated with the ratio $\sigma^2(2)/\sigma^2(N)$ depends upon m . The derivation of this is more complex than that for the individual terms given above in Eqs. (20) and (21) and therefore a Monte Carlo simulation was used. The results of a comprehensive exploration indicated that the values of r for the ratio, or $\Gamma + 1$, were in fact indistinguishable from those for the Allan variance alone, i.e., Eq. (19).

Because the value of r_{ij} is less than unity, there will be some gain in precision through use of subsets. If measurements are gathered into groupings of, say, 2, 4, 8, etc., then the values of r_{12} , r_{14} , and r_{18} are 0.354, 0.125, and 0.044, respectively. Although the Allan variance for the different groupings show some correlation, it is seen to be short ranged and weak.

In a weighted least-squares fit in which the data are concatenated into sets differing in number by factors of 2, the error matrix for large n takes the form

$$\begin{pmatrix} \sigma_{11}^2 & 0.354\sigma_{11}\sigma_{22} & 0.125\sigma_{11}\sigma_{33} & 0.044\sigma_{11}\sigma_{44} \\ 0.354\sigma_{11}\sigma_{22} & \sigma_{22}^2 & 0.354\sigma_{22}\sigma_{33} & 0.125\sigma_{22}\sigma_{44} \\ 0.125\sigma_{11}\sigma_{33} & 0.354\sigma_{22}\sigma_{33} & \sigma_{33}^2 & \dots \\ \dots & \dots & \dots & \dots \end{pmatrix}.$$

The use of similarly grouped but totally independent data would have only the diagonal terms. Comparison of the results obtained for two such cases is displayed in Fig. 7 where a set of 2048 normally distributed observations are treated.

The principal graph shows how the variance in C depends upon the degree of gathering or, when independent data are used, how the measurements are made. The error is seen to reach a minimum in the region of 16, i.e., 16 sets each consisting of 128 observations. The error grows as the number of sets either increases or decreases. If one were to use only a single optimum value, the variance in C would be $5.7/Z^2$, where Z is the number of total counts.

The inset in Fig. 7 shows how the error depends upon the number of groupings one uses when the data are independent or when derived from a single set, as is the case here. For this figure the ratio of m values were always selected to be in constant ratio, i.e., 1, 2, 3, 8, 16, 32, etc. Naturally the error for the independent data decreases with increasing number of sets, since these require additional measurements. The error for the single data set approaches a limiting value of $1.86/Z^2$ as the number of groups increases. This figure shows that the error is $2/Z^2$ when groups differ in size by a factor of 2. Thus, although the data are correlated, a gain in precision can be realized through use of grouping. In addition, the subjectivity of selecting a particular grouping is avoided. Details of the method used to analyze the observations follows.

For the set of groupings used, values of C_m were calcu-

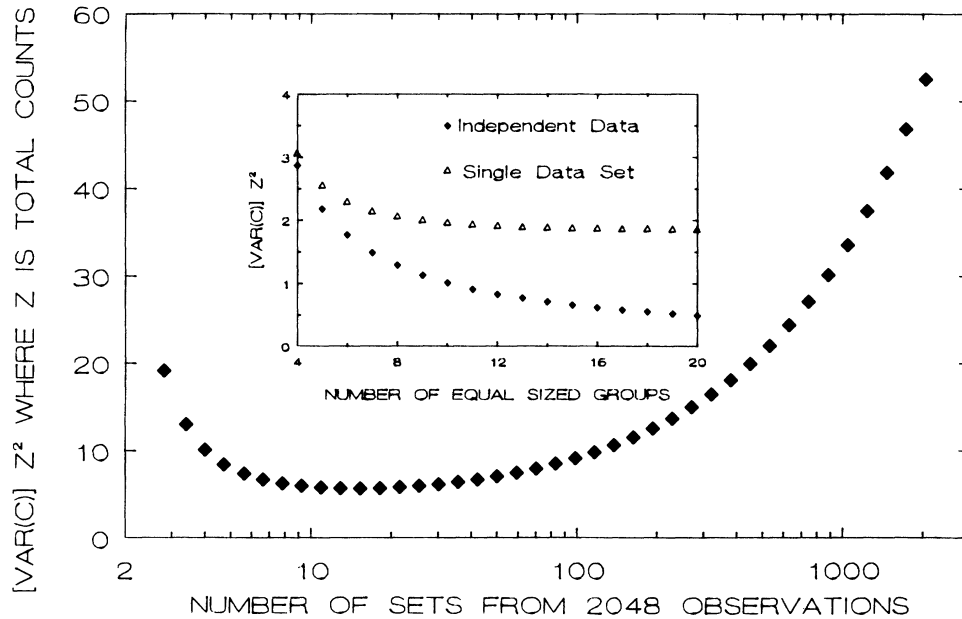


FIG. 7. Effect on the error is portrayed as a function of how observations are grouped into sets. The inset shows how the error is affected as 2048 observations are lumped into a variety of equal-sized groups. The independent data show continual error reduction with finer division since each represents a complete set of measurements. The single data set levels off because of the correlation between the groupings. Here a low value of error is reached with 9 sets, i.e., factors of about 2. The main graph shows that the precision for estimation of C is highest for 10–20 sets. These curves indicate that one should use data sets of 4,8,16,...,1024 and 2048 members.

TABLE I. Summary of results. (a) Run 1. Mean counts: total area is 18 648 687 per observation, window area 18 354 605 per observation. Total number of 30-min observations is 1696. (b) Run 2. Mean counts: total area is 18 647 020 per observation, window area is 18 354 602 per observation. Total number of 30-min observations is 2048. The final grand average for (a) and (b) is $\langle C \rangle = (1.5 \pm 2.7) \times 10^{-11}$.

Number of sets	Members per set	Total spectral area			Window sepctral area		
		$\sigma^2(2)/\sigma^2(N)$	$C \times 10^{11}$	$\sigma_C \times 10^{11}$	$\sigma^2(2)/\sigma^2(n)$	$C \times 10^{11}$	$\sigma_C \times 10^{11}$
(a)							
1696	1	0.954	43.19	21.5	0.942	55.32	21.8
848	2	1.007	-3.47	17.1	0.979	10.78	17.4
424	4	1.017	-4.78	13.9	0.989	3.20	14.1
212	8	0.993	1.19	11.5	1.002	-0.33	11.7
106	16	1.008	-0.80	9.7	1.012	-1.19	9.9
53	32	1.049	-2.87	8.5	0.939	4.24	8.6
32	53	0.837	10.26	7.9	0.828	11.04	8.0
16	106	1.320	-6.43	7.5	1.296	-6.12	7.7
8	212	1.200	-3.45	7.9	1.053	-1.20	8.0
4	424	1.689	-5.02	10.0	1.596	-4.82	10.2
$\langle C \rangle = (-0.36 \pm 4.44) \times 10^{-11}$				$\langle C \rangle = (2.13 \pm 4.51) \times 10^{-11}$			
(b)							
2048	1	1.046	-38.01	19.0	0.939	57.53	19.3
1024	2	1.056	-25.68	15.1	0.948	27.27	15.3
512	4	0.956	13.06	12.2	0.903	31.03	12.4
256	8	0.858	28.53	10.0	0.913	16.03	10.1
128	16	1.019	-1.80	8.4	0.874	14.86	8.5
64	32	1.289	-12.12	7.3	0.790	18.32	7.4
32	64	1.012	-0.46	6.5	1.125	-4.03	6.7
16	128	1.550	-7.32	6.2	0.955	1.33	6.3
8	256	1.068	-1.26	6.5	1.600	-5.29	6.6
4	512	1.650	-4.16	8.3	1.300	-3.14	8.4
$\langle C \rangle = (-2.65 \pm 3.67) \times 10^{-11}$				$\langle C \rangle = (6.77 \pm 3.73) \times 10^{-11}$			

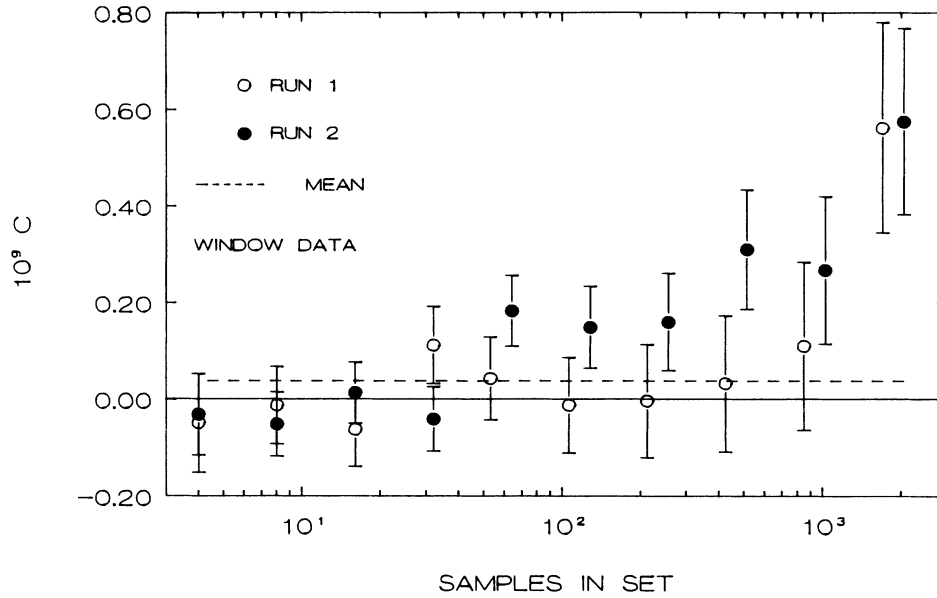


FIG. 8. Value of C is shown for the various sets. The data used are for the window area. The dashed line is the mean for both run 1 and 2.

lated for each group from the observed ratio $\sigma^2(2)/\sigma^2(N)$. Because the ratio is very close to unity as indicated by Figs. 5 and 6, the value of Γ in the error estimation, Eq. (10), was taken to be zero when evaluating σ_C^2 . These errors form the diagonal elements in the error matrix. Based upon the m values, the off-diagonal elements were determined using Eq. (19) and the diagonal terms.

The objective then is to find the value of C that minimizes the quantity

$$\chi^2 = \sum_{i=1}^s \frac{(C_i - C)^2}{\sigma_i^2} \tag{22}$$

where $\sigma_i^2 = \sigma_{ii}^2$. For the s terms involved, solution yields the condition

$$C = \frac{\sum_{i=1}^s C_i / \sigma_i^2}{\sum_{i=1}^s 1 / \sigma_i^2} \tag{23}$$

Proceeding to find the error associated with this estimate

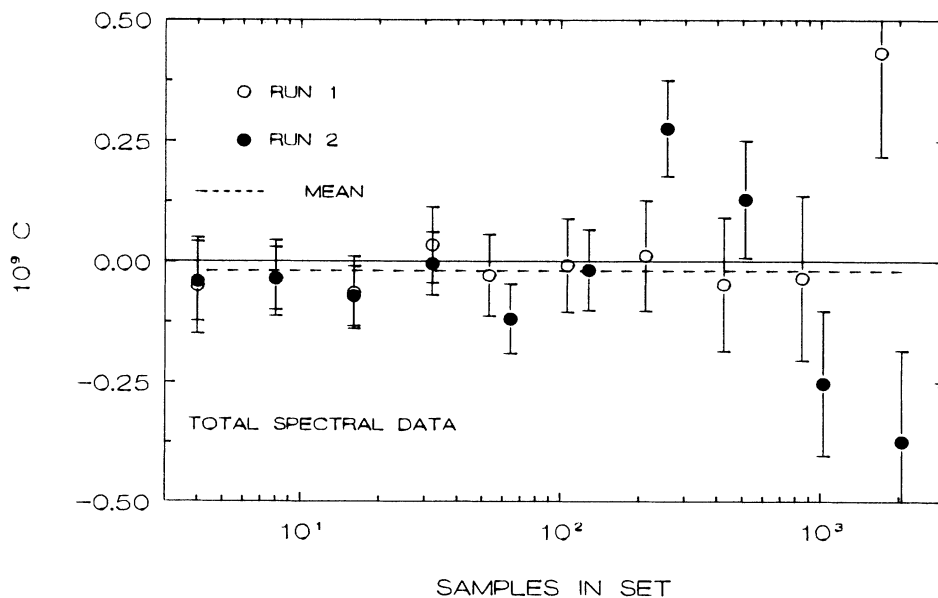


FIG. 9. Data for the total area displayed in a manner similar to that of Fig. 8.

of C using error propagation gives

$$\sigma^2(C) = \sum_{i=1}^s \sum_{j=1}^s (\sigma_{ij}^2 / \sigma_i^2 \sigma_j^2) / \left(\sum_{i=1}^s 1/\sigma_i^2 \right)^2. \quad (24)$$

A summary of the input data for this treatment is given in Table I. Plots of the results for C are given in Figs. 8 and 9. Figure 8 shows the relationship between C and the samples per set using the window generated data while Fig. 9 shows that found for the total area method of analysis.

The errors quoted for the average values for C in Table I include that from the covariance. For both runs, two estimates are found which, while they can be used in averaging, cannot be combined to reduce the error because of correlation. The final result is then $C = (1.5 \pm 2.7) \times 10^{-11}$. This corresponds to a "flicker floor" of $F = (2.1 \pm 3.7) \times 10^{-11}$.

DISCUSSION AND CONCLUSIONS

The present findings do not support the contention that there is a $1/f$ contribution in α decay but rather that the process is completely described by Poisson statistics. The chance that the value of F is 10^{-7} is clearly

outside the realm of possibility. The greatest difficulty in establishing a very low limit for a second process is that of controlling the stability of experimental factors. Because of the additive nature of second moments, positive results most frequently reflect poor experimental conditions.

Further reduction of the limit established here requires either a significant increase in the counting time or in the counting rate. To reduce C by another order of magnitude using the current arrangement would require 2.3 yr of continuous counting. The same result could be obtained in a week if a counting rate of about 10^6 is used. Retaining the scintillator method would require the use of a material with much faster decay time than NaI(Tl). Unfortunately, plastic scintillators which have fast decay times display a rather low light output for α particles in comparison to electrons. We are currently exploring options, however, the limit now placed upon C would seem to dispel the claims made by the earlier investigators.⁹⁻¹¹

ACKNOWLEDGMENTS

The authors wish to thank the Natural Sciences and Engineering Research Council for their financial support.

-
- ¹J. S. Barnes and S. Jarvis Jr., National Bureau of Standards Technical Note No. 604, 1971 (unpublished).
²P. H. Handel, Phys. Rev. Lett. **34**, 1492 (1975).
³P. H. Handel, Phys. Rev. A **22**, 745 (1980).
⁴A. van der Ziel, Proc. IEEE **76**, 233 (1988).
⁵C. M. van Vliet and P. H. Handel, Physica (Utrecht) **113A**, 261 (1982).
⁶P. Dutta and P. M. Horn, Rev. Mod. Phys. **53**, 497 (1981).
⁷R. D. Black, IEEE Trans. Electron Devices **ED-33**, 532 (1986).
⁸Th. M. Nieuwenhuizen, D. Frenkel, and N. G. van Kampen, Phys. Rev. A **35**, 2750 (1987).
⁹J. Gong, C. M. van Vliet, G. Bosman, and P. H. Handel, *Noise in Physical Systems and 1/f Noise*, edited by M. Savelli, G. Lecoy, and J. P. Nougier (Elsevier, New York, 1983), p. 381.
¹⁰G. S. Kousik, J. Gong, C. M. van Vliet, G. Bosman, W. H. Ellis, and E. E. Carroll, *Noise in Physical Systems and 1/f Noise*, edited by A. D'Amico and P. Mazzetti (Elsevier, New York, 1986).
¹¹G. S. Kousik, J. Gong, C. M. van Vliet, G. Bosman, W. H. Ellis, and E. E. Carroll, Can. J. Phys. **65**, 365 (1986).
¹²W. V. Prestwich, T. J. Kennett, and G. T. Pepper, Phys. Rev. A **34**, 5132 (1986).
¹³W. V. Prestwich, T. J. Kennett, and G. T. Pepper, Can. J. Phys. **66**, 100 (1988).
¹⁴G. T. Pepper, T. J. Kennett, and W. V. Prestwich, Can. J. Phys. **67**, 468 (1989).
¹⁵J. A. Barnes, Proc. IEEE **54**, 207 (1966).
¹⁶D. W. Allan, Proc. IEEE **54**, 221 (1966).
¹⁷H. V. Malmstadt, C. G. Enke, S. R. Couch, and G. Horlick, *Electronic Measurements for Scientists* (Benjamin, New York, 1974), p. 734.
¹⁸A. Robertson, W. V. Prestwich, and T. J. Kennett, Nucl. Instrum. Methods **100**, 317 (1972).
¹⁹C. M. Lederer and V. S. Shirley, *Table of the Isotopes* (Wiley, New York, 1978).
²⁰C. H. Vicent, *Random Pulse Trains*, Vol. 13 of IEE Monograph Series (Peter Peregrinus, London, 1973), p. 96.
²¹J. von Neumann, Ann. Math. Stat. **12**, 367 (1941).
²²J. Durbin and G. S. Watson, Biometrika **37**, 409 (1950).
²³J. D. Williams, Ann. Math. Stat. **12**, 239 (1941).